



## RF Plasma Nitriding of AISI 304 Stainless Steel

Sun Kyu Kim<sup>a\*</sup>, Jung Sik Yoo<sup>b</sup>, Matthew P. Fewell<sup>c</sup>

<sup>a</sup>Traditional Technology Innovation Research Laboratory

School of Materials Science and Engineering,

University of Ulsan, Ulsan 680-749, Korea

<sup>b</sup>LG CNS, 642-3, Jinpyung-dong, Gumi, Gyoungbuk 730-726, Korea

<sup>c</sup>Physics and Electronic Engineering, University of New England,  
 Armidale NSW 2351, Australia

(Received 27 November 2003 ; accepted 7 January 2004)

### Abstract

Austenitic stainless steel AISI 304 was nitrided in a low-pressure RF plasma using pure nitrogen. With a treatment of time of 4.0 h at 400°C, the nitrogen-rich layer on the sample was 3 μm thick and had a hardness of approximately 4.4 times higher than that of untreated material. XRD data showed that as the process temperature rose from 350~450°C, the expanded austenite peaks became more prominent while the austenite peaks became weaker. Expanded austenite was transformed to ferrite and CrN at the treatment of 500°C. Langmuir probe measurements showed that electron density decreased above 450°C.

*Keywords* : RF plasma nitriding, Austenitic stainless steel, AISI 304, Expanded austenite

### INTRODUCTION

Plasma nitriding is a plasma-activated thermochemical method for increasing the surface hardness and wear resistance of metals. Commercial plasma-nitriding reactors use an abnormal glow discharge, either dc or pulsed. They perform well when nitriding low-alloy<sup>1)</sup> and tool steels, but they are less successful with stainless steel, particularly those grades with an austenitic structure. The high treatment temperature common in commercial nitriding processes causes precipitation of CrN<sup>2)</sup>, resulting in surfaces that are hard and resistant to wear but suffer degraded corrosion resistance. The use of lower treatment temperatures<sup>2,3)</sup> and low-pressure discharges<sup>4)</sup> has been found to be effective in addressing this problem. The modified layer so produced contains a phase, sometimes called S-phase or expanded austenite, that is very rich in nitrogen. A similar phase can be produced by ion implantation<sup>5)</sup> and by reactive sputtering<sup>6)</sup>.

Low-pressure RF plasma is the basis of plasma-immersion ion implantation. In the context of the

treatment of steels at elevated temperatures, this can be thought of as a nitriding process with the addition of high-energy (20~50 keV) ion bombardment<sup>7)</sup>. Thus, the study of RF nitriding provides insight into the underlying plasma behavior in process like plasma immersion ion implantation.

Several other considerations also provide motivation for a study of RF plasmas in the context of nitriding. Gas pressures can be much lower in RF plasmas than in DC glows, leading to lower consumption of feed gas. Also, by using an antenna other than the workpiece, plasma generation is separated from substrate bias, thus removing the need for arc suppression and allowing better control of the process.

The plasma nitriding of AISI 316 stainless steel has been studied much<sup>8,9)</sup>. There is a need for working on other grade stainless steels. This paper reports results from a study of the nitriding of AISI 304 stainless steel by RF plasma in pure nitrogen.

### EXPERIMENTAL

The AISI 304 alloy (C<0.08, Si<1.00, P<0.045, S<0.030, Cr 19.0, Mn<2.00, Ni 9.0, balance: Fe) was

\*Corresponding author. E-mail : skim@mail.ulsan.ac.kr

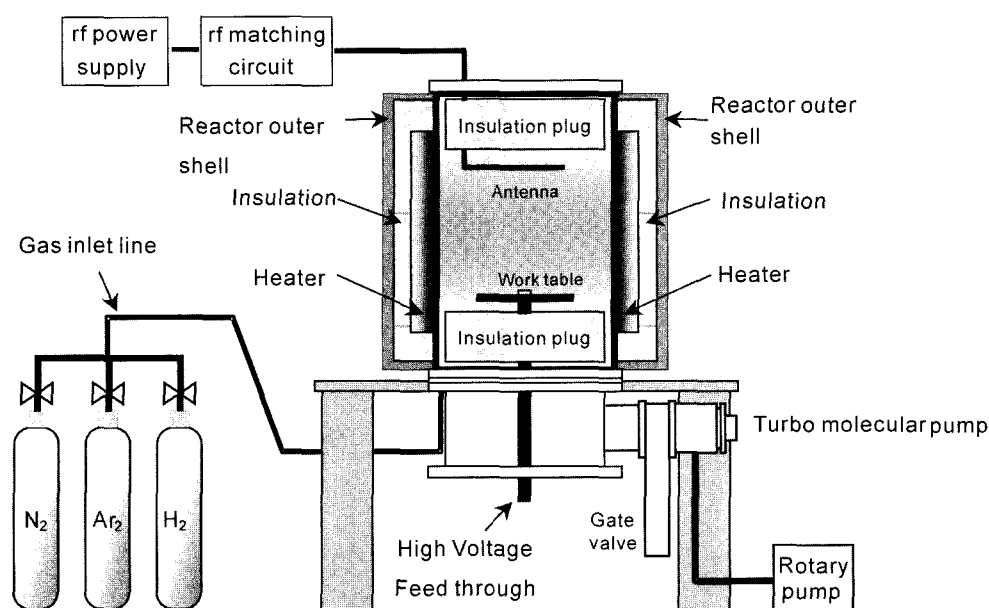


Fig. 1. Schematic diagram of experimental apparatus.

used for the samples. The samples consisted of disks 25 mm in diameter and 4 mm thick, which were surface ground, polished and ultrasonically cleaned in ethanol prior to loading onto the sample table of the hot-wall nitriding reactor at the Australian Nuclear Science and Technology Organization (ANSTO). The schematic diagram of the apparatus is shown in Fig. 1. This reactor is fabricated from stainless steel and pumped by a large-capacity turbomolecular pump. A single-turn inductively coupled antenna, also made from stainless steel, is located inside the reactor volume. At an appropriate gas pressure, a diffuse RF glow discharge fills the reactor when RF power is applied to the antenna.

The sample table of the hot-wall reactor can accommodate several samples in one loading. Four treatments used the process temperature of 400°C, with treatment time varied in the range 1~16 h, and four treatments used a process time of 4 h, with temperature in the range 350~500°C. All treatments included a precleaning step: the reactor was filled with a 50/50 mixture of hydrogen and argon, and as RF glow discharge was maintained as the sample was heated to the process temperature. The length of time required for this varied in the range 1.5~2.0 h depending on the desired process temperature and the temperature of the reactor walls at the beginning of the day. At the end of the precleaning, the chamber was pumped out and filled with nitrogen for the nitriding step. During all plasma exposure, both precleaning and nitriding, the sample was biased at -250 V with respect to the reactor walls. Following the treatment, the samples

Table 1. Process parameters used in this study

	Precleaning	Nitriding
rf power and frequency	250 W at 13.56 MHz	
Total pressure (mPa)	400	400
Sample bias (V)	-250	-250
Time (h)	1.5~2.0	1.0~16.0
H <sub>2</sub> flow rate ( $\mu\text{mol s}^{-1}$ )*	11.9	-
N <sub>2</sub> flow rate ( $\mu\text{mol s}^{-1}$ )	-	11.0
Ar flow rate ( $\mu\text{mol s}^{-1}$ )	3.8	0

\*1.0  $\mu\text{mol s}^{-1}$  = 1.36 sccm

were cooled under vacuum conditions. The ranges of treatment parameters used for samples studied herein are given in Table 1.

In the hot-wall reactor, the whole volume is at the working temperature, which was monitored by both a thermocouple and an optical pyrometer. The uncertainty on the temperature is  $\pm 10^\circ\text{C}$ . As indicated in Table 1, all steps of the process use flowing gas. The system shows differential pumping, with hydrogen being pumped the most efficiently: this was allowed prior to the treatments by noting the relationship between pressure for each gas separately. The glow rates given in the middle column of Table 1 produce an H<sub>2</sub>/Ar mixture with equal partial pressures of the two gases.

Following the treatments, the samples were examined by x-ray diffractometry (XRD) and scanning electron microscopy (SEM), and their surface hardness was measured by an instrumented method. The X-ray diffractometry was performed on the Phillips PW

1050 diffractometer located at the University of New England, using Cu K radiation and Bragg Brentano geometry. Scanning electron microscopy (SEM) was used to image the treated layer. A thin cross-sectional slice was cut from each sample and cast in epoxy resin. This was then surface ground and polished. To render the nitrogen-rich layer visible, the polished surface was chemically etched for 10s in Marble's solution (10 g copper sulphate in 100 ml of 6.0 M hydrochloric acid). Finally, the etched sample was coated with carbon to reduce the charging that generally occurs during SEM analysis of metallic samples cast in insulating materials. Examination of these samples was carried out in the (JEOL, JSM-820) scanning electron microscope located at the University of Ulsan. Measurements of the surface hardness of the samples were made with the Nano instrumented indenter located at ANSTO, using loads of 0.05 N, 0.25 N and 1.0 N. Five measurements were made on each sample at each load; uncertainties are taken as the standard deviation of each set of measurements. The Langmuir probe was used for measurement of the local properties of plasma. A single cylindrical collecting-probe was used.

## RESULTS

Fig. 2 shows X-ray diffractograms from the AISI 304 samples. Fig. 2(a) shows, as the process temperature rises from 350°C-450°C, the peaks from the underlying austenite become weaker and the expanded austenite peaks more prominent as the thickness of the treated layer increases. The diffractogram from the treatment at 500°C is quite different, showing that the well known transformation from expanded austenite to ferrite and CrN has occurred. Similar remarks apply to Fig. 2(b), which is consistent with thicker treated layers after longer treatment time. The increasing treatment time indicates an increasing expansion of the lattice presumably due to an increasing nitrogen content. The most interesting feature in Fig. 2 is the double structure shown by the expanded austenite peaks in Fig. 2(b) for the sample treated at 400°C for 1.0 h. This is reminiscent of results reported by Czerwicz *et al.*<sup>10)</sup> in AISI 316 and attribute to a two-component structure for the nitrogen-rich layer.

Fig. 3 shows the result of instrumented indentation, parallel to Fig. 2. In Fig. 3, the variation of measured hardness of the treated samples with indenter load reflects the effect of a thin hard layer on a softer substrate. Electron micrographs of the cross section

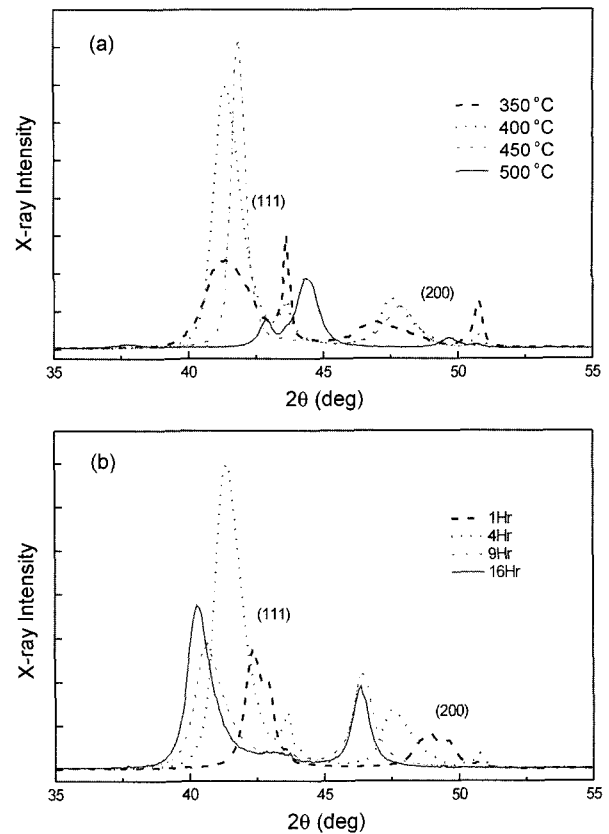


Fig. 2. X-ray diffractograms of AISI 304 samples nitrided (a) for 4 h at the temperatures indicated and (b) at 400°C for the lengths of time indicated.

of an indent in AISI 316 stainless steel show that, at an indenter load of 1.0 N, the highest load used here, the treated layer is not punctured but is driven into the softer substrate. The hardness value obtained is therefore intermediate between the true hardness of the treated layer and the hardness of the substrate. Hence, the values at the lightest load (0.05 N) give the best indication of the hardness of the treated layer. The results at 1.0 N load can be regarded as reflecting the thickness of the treated layer; the trends shown in Fig. 3 support the conclusion from XRD.

Fig. 4 shows SEM micrograph of cross-section of nitrided layer of AISI 304 samples. A nitrided layer of about 3  $\mu\text{m}$  was formed.

Hot-wall nitriding reactor is more efficient than cold-wall nitriding reactor since the hot-wall vacuum furnace favors production of higher densities of electrons, molecular ions and metastable energy levels of the nitrogen molecule. To investigate the effect of this phenomenon on the low-pressure RF nitriding plasma, an investigation of the plasma process parameter space with temperature was undertaken

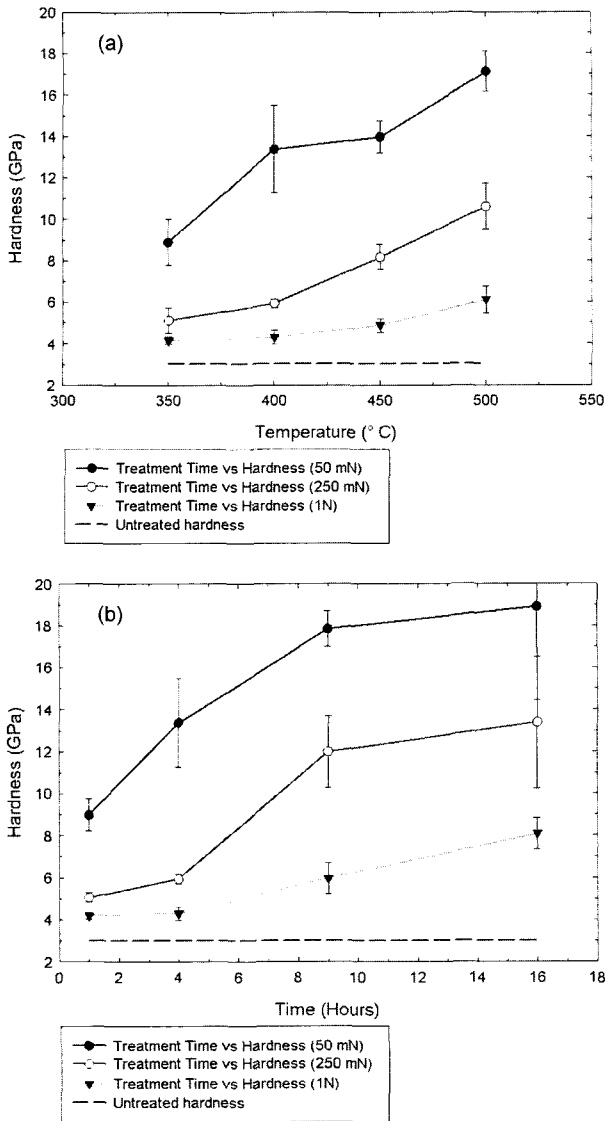


Fig. 3. Measurement of surface hardness by nano-indentation for AISI 304 samples nitrided (a) for 4 h at the temperatures indicated and (b) at 400°C for the lengths of time indicated.

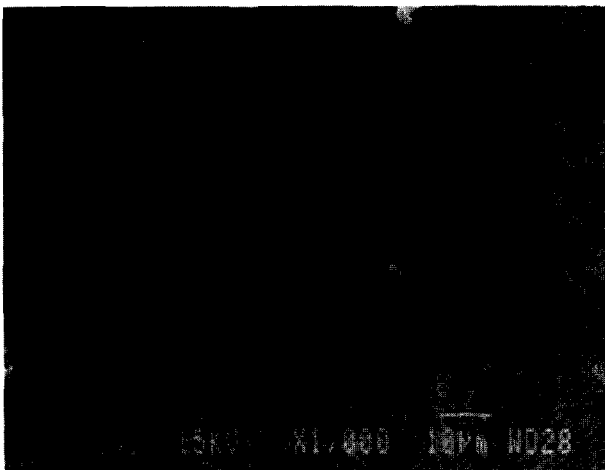


Fig. 4. SEM micrograph of cross-section of nitrided layer.

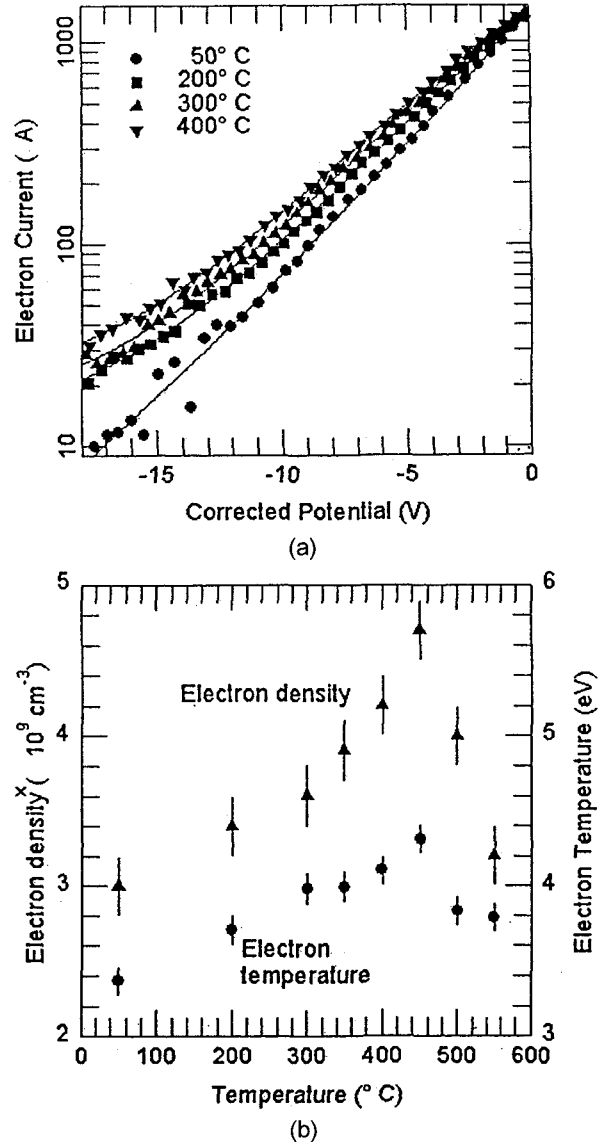


Fig. 5. Results of Langmuir-probe measurements (a) Electron current measurements as a function of corrected potential for process temperatures varying from 50–400°C and at a pressure of 400 mPa and 250W RF power (b) Electron density (triangles) and electron temperatures (circles) as a function of process temperature.

within the hot-wall nitriding reactor. During treatment the conditions within the plasma were characterized by Langmuir-probe measurements. Fig. 5 shows results of Langmuir-probe studies. Fig. 5(a) shows comparison of a selection of current-voltage characteristics for various process temperatures in the hot-wall reactor, while Fig. 5(b) shows the electron density and average electron energy as a function of process temperature. These data were taken in a 250 W RF plasma at a constant pressure of 400 mPa with the sample table biased at  $-250^{\circ}\text{C}$ . Fig. 5(a) shows the electron current as a function of corrected potential: that is the positive-

ion current has been subtracted so that the abscissa represents probe bias with respect to the plasma potential. The results indicated that, as the temperature was increased, both the average electron energy (proportional to the reciprocal of the slope) and the number of collected electrons increased. This is most distinct for the largest negative corrected potentials, indicating a higher proportion of high-energy electrons (above 10 eV) in the plasma. It is interesting to note the correlation between the results of Baldwin<sup>8)</sup> and these data for process temperatures above 450°C. Baldwin found that as the temperature was increased above 450°C, metastable-particle induced electron production decreased. This is a trend that is also reflected in the electron density measurements of Fig. 5(b). This phenomenon can be explained in terms of the surface properties of stainless steel with temperature. The migration of Cr from solid solution at room temperatures above 450°C leads to the formation of CrN which could give sufficient change in the surface properties and thus the workfunction of the material.

## CONCLUSION

A low-pressure RF discharge using pure nitrogen is an effective medium for nitriding austenitic stainless steel. With a treatment time of 4.0 h at 400°C, The nitrogen-rich layer was 3 μm thick and has a hardness about 4.4 times higher than that of untreated material. As the process temperature rose from 350~450°C, the peaks from the underlying austenite became weaker and the expanded austenite peaks became more prominent. Transformation from expanded austenite

to ferrite and CrN occurred at 500°C. Langmuir probe measurements showed that electron density decreased above 450°C.

## ACKNOWLEDGEMENT

This research was supported by the 2003 University of Ulsan Research Fund.

## REFERENCES

1. K.-T. Rie, E. Menthe, A. Matthews, K. O. Leggs, J. Chin, *MRS Bull.*, 21 (1996) 46.
2. Z. L. Zhang, T. Bell, *Surf. Eng.*, 1 (1985) 131.
3. E. Menthe, K.-T. Rie, J. W. Schutze, S. Simmons, *Surf. Coat. Technol.*, 7475 (1995) 412.
4. G. A. Collins, R. Hutchings, K. T. Short, J. Tendys, X. Li, M. Samandi, *Surf. Coat. Technol.*, 7475 (1995) 417.
5. D. L. Williamson, O. Ozturk, R. Wei, P. J. Wilbur, *Surf. Coat. Technol.*, 65 (1994) 14.
6. A. Saker, Ch. Leroy, H. Michel, E. Frantz, *Mater. Sci. Eng. A*, 140 (1991) 702.
7. G. A. Collins, R. Hutchings, J. Tendys, *Surf. Coat. Technol.*, 59 (1993) 267.
8. M. J. Baldwin, M. P. Fewell, S. C. Haydon, S. Kumar, G. A. Collins, *Surf. Coat. Technol.*, 98 (1998) 1187.
9. J. M. Priest, M. J. Baldwin, M. P. Fewell, S. C. Haydon, G. A. Collins, K. T. Short, J. Tendys, *Thin Solid Films*, 345 (1999) 113.
10. T. Czerwiec, N. Renevier, H. Michel, *Surf. Coat. Technol.*, 133 (2000) 267.